Microstructure of $LiCoO_2$ with and without "$AlPO_4$" Nanoparticle Coating: Combined STEM and XPS Studies

Anjuli T. Appapillai,[†] Azzam N. Mansour,[‡] Jaephil Cho,[§] and Yang Shao-Horn*,[†]

Massachusetts Institute of Technology, Cambridge, Massachusetts 02139, Naval Surface Warfare Center, Carderock Division, West Bethesda, Maryland 20817-5700, and Kumoh National Institute of Technology, Gumi, Republic of Korea

Received June 8, 2007. Revised Manuscript Received August 1, 2007

"$AlPO_4$"-coated $LiCoO_2$ was shown to exhibit markedly improved capacity retention relative to bare $LiCoO_2$ upon cycling to 4.7 V. Scanning and transmission electron microscopy imaging showed that the coating thickness of "$AlPO_4$"-coated $LiCoO_2$ varied from ∼10 to ∼100 nm. Energy-dispersive X-ray mapping revealed that the coating was not single-phase "$AlPO_4$", rather consisting of P-rich thick regions (∼100 nm) and Al-rich thin regions (∼10 nm). Detailed X-ray photoelectron spectroscopy (XPS) studies of the "$AlPO_4$"-coated $LiCoO_2$ in comparison to bare $LiCoO_2$ and various reference compounds such as Li_2CO_3, Li_3PO_4, and $AlPO_4$ indicate that (1) $AlPO_4$ is absent on the surface; (2) the surface consisted of Li_3PO_4 and heavily Al substituted $LiAl_yCo_{1-y}O_2$, which may result from $AlPO_4$ nanoparticles reacting with bare $LiCoO_2$ during the coating heat treatment at 700 °C; and (3) the amount of surface Li_2CO_3 is markedly reduced in the coated sample relative to the bare $LiCoO_2$. The existence of Li_3PO_4 in "$AlPO_4$"-coated $LiCoO_2$ was confirmed with X-ray powder diffraction. The coating microstructure of "$AlPO_4$"-coated $LiCoO_2$ is proposed, and the mechanisms of enhancement in the cycling and thermal characteristics by particle surface microstructure are discussed in detail.

Introduction

Lithium cobalt dioxide, $LiCoO_2$, is the most common positive electrode material used in lithium rechargeable batteries for portable electronics. $LiCoO_2$ adopts a layered structure having rhombohedral symmetry with space group $R\bar{3}m$, which is described typically in a hexagonal cell setting with $a_{hex} = 2.815$ Å and $c_{hex} = 14.05$ Å.[1] The structure consists of layers of edge-sharing lithium and cobalt octahedra stacked alternatively between AB CA BC cubic-close-packed oxygen arrays. The theoretical capacity of $LiCoO_2$ is 274 mA h g^{-1} for reversible extraction and insertion of one lithium per formula unit. However, cycling to voltages greater than 4.2 V (which corresponds to removal of ∼0.5 Li per formula unit) has shown severe capacity loss.[2,3] Two major causes have been proposed for the capacity fade: (1) structural instability[2,4,5] (such as microcracks induced by dimensional changes as a function of Li content) and (2) the surface instability as a result of Li_xCoO_2 reactivity with the electrolyte[2] (such as cobalt dissolution) of the $LiCoO_2$ crystals. Al substitution in $LiCoO_2$ has been shown to be particularly effective in improving capacity retention upon cycling by not only reducing changes in the lattice parameters of the layered Li_xCoO_2 structure[6,7] but also decreasing cobalt dissolution.[6] However, Al substitution reduces rechargeable capacities of $Li_xAl_yCo_{1-y}O_2$ as Al^{3+} in the layered structure is not electroactive. Recently, researchers have shown that application of a surface oxide or phosphate such as ZrO_2,[8] Al_2O_3,[8−10] TiO_2,[8,11] and $AlPO_4$[12] to $LiCoO_2$ particles can significantly improve the degree of capacity retention upon cycling to high voltages without loss in the reversible capacity. In particular, "$AlPO_4$"-coated $LiCoO_2$ as reported by Cho et al.[12−19] has shown superior cycling performance

* Corresponding author. E-mail: shaohorn@mit.edu.
[†] Massachusetts Institute of Technology.
[‡] Naval Surface Warfare Center.
[§] Kumoh National Institute of Technology.

(1) Orman, H. J.; Wiseman, P. J. *Acta Crystallogr., Sect. C* **1984**, *40*, 12−14.
(2) Amatucci, G. G.; Tarascon, J. M.; Klein, L. C. *Solid State Ionics* **1996**, *83*, 167−173.
(3) Aurbach, D. *J. Power Sources* **2000**, *89* (2), 206−218.
(4) Ohzuku, T.; Ueda, A. *J. Electrochem. Soc.* **1994**, *141* (11), 2972−2977.
(5) Wang, H. F.; Jang, Y. I.; Huang, B. Y.; Sadoway, D. R.; Chiang, Y. T. *J. Electrochem. Soc.* **1999**, *146* (2), 473−480.
(6) Myung, S. T.; Kumagai, N.; Komaba, S.; Chung, H. T. *Solid State Ionics* **2001**, *139* (1−2), 47−56.
(7) Jang, Y. I.; Huang, B. Y.; Wang, H. F.; Sadoway, D. R.; Ceder, G.; Chiang, Y. M.; Liu, H.; Tamura, H. *J. Electrochem. Soc.* **1999**, *146* (3), 862−868.
(8) Kim, Y. J.; Cho, J. P.; Kim, T. J.; Park, B. *J. Electrochem. Soc.* **2003**, *150* (12), A1723−A1725.
(9) Oh, S.; Lee, J. K.; Byun, D.; Cho, W. I.; Cho, B. W. *J. Power Sources* **2004**, *132* (1−2), 249−255.
(10) Cho, J.; Kim, Y. J.; Park, B. *Chem. Mater.* **2000**, *12*, 3788.
(11) Fey, G. T. K.; Lu, C. Z.; Huang, J. D.; Kumar, T. P.; Chang, Y. C. *J. Power Sources* **2005**, *146* (1−2), 65−70.
(12) Cho, J.; Kim, Y. W.; Kim, B.; Lee, J. G.; Park, B. *Angew. Chem., Int. Ed.* **2003**, *42* (14), 1618−1621.
(13) Cho, J. *Electrochim. Acta* **2003**, *48* (19), 2807−2811.
(14) Kim, B.; Lee, J. G.; Choi, M.; Cho, J.; Park, B. *J. Power Sources* **2004**, *126* (1−2), 190−192.
(15) Cho, J.; Kim, T. G.; Kim, C.; Lee, J. G.; Kim, Y. W.; Park, B. *J. Power Sources* **2005**, *146* (1−2), 58−64.
(16) Cho, J. P.; Kim, B.; Lee, J. G.; Kim, Y. W.; Park, B. *J. Electrochem. Soc.* **2005**, *152* (1), A32−A36.
(17) Kim, J.; Noh, M.; Cho, J.; Kim, H.; Kim, K. B. *J. Electrochem. Soc.* **2005**, *152* (6), A1142−A1148.
(18) Cho, J.; Lee, J. G.; Kim, B.; Kim, T. G.; Kim, J.; Park, B. *Electrochim. Acta* **2005**, *50* (20), 4182−4187.
(19) Lee, J. G.; Kim, B.; Cho, J.; Kim, Y. W.; Park, B. *J. Electrochem. Soc.* **2004**, *151* (6), A801−A805.

10.1021/cm0715390 CCC: $37.00
Published on Web 10/13/2007

relative to $LiCoO_2$ coated with other oxides. Specifically, the $AlPO_4$ coating has been shown to increase the initial reversible discharge capacity from 200 to 210 mA h g^{-1} with a 4.8 V upper limit,[18] and "$AlPO_4$"-coated $LiCoO_2$ electrodes retain ~150 mA h g^{-1} in capacity after 50 cycles.[19] Moreover, "$AlPO_4$"-coated $LiCoO_2$ exhibits markedly improved thermal stability relative to uncoated $LiCoO_2$ and $LiCoO_2$ with oxide coating.[15] In a charged state of 4.7 V, "$AlPO_4$"-coated $LiCoO_2$ increases the onset temperature for electrolyte oxidation from 187 to ~220 °C, and reduces the overall heat evolution by a factor of 10.[13]

The mechanism of the improvement in cycling performance and thermal characteristics of lithium transition metal oxides with $AlPO_4$ and other oxides is not well-understood. Cho et al.[20,21] have first proposed that increasing the fracture toughness of the coating oxide (e.g., Al_2O_3 and ZrO_2) can suppress phase transitions by constraining active particles against lattice parameter changes associated with lithium removal and insertion, which would reduce stresses and structural damage within individual particles and improve capacity retention during cycling. This concept is further supported by Fey et al. using slow-scan cyclic voltammetry data with an upper voltage limit of 4.4 V, which show that the phase transition peaks are suppressed to varying degrees that are dependent on the coating material.[22,23] However, Chen and Dahn[24] show that coating does not suppress the changes in the lattice parameters of the layered structure upon lithium removal and insertion, and the enhancement in cycling performance is independent of fracture toughness of the coating. This argument is in good agreement with recent findings of Cho et al., where it is shown that suppression of lattice expansion is not necessary to obtain improved cycling performance of "$AlPO_4$"-coated $LiCoO_2$ in contrast to oxide coatings. Chen and Dahn[25] have also shown that a heat treatment to 550 °C alone can improve the reversible capacity and capacity retention of Li_xCoO_2 electrodes when cycled to 4.5 V by reducing moisture-related, surface, chemical species. Although coating application typically involves a heat-treatment step, this explanation does not explain the difference in cycling performance of lithium cobalt oxide electrode materials with different coatings.[15] The mechanism by which coating may influence thermal characteristics of Li_xCoO_2 is not known. Although Cho et al.[12] have speculated that the superior thermal properties of "$AlPO_4$"-coated $LiCoO_2$ is attributed to the strong covalency of the PO_4 polyanions with the Al^{3+} ions of the coating, ambiguity exists in the chemistry and microstructure of the $AlPO_4$ coating. Cho et al.[21] and Kim et al.[26] have shown that coating nanoparticles can react with bare $LiCoO_2$ during the heat-treatment step, which may lead to considerably different surface microstructure and chemistry from pristine coating particles. Therefore, it is important to reveal the surface microstructure of coated Li_xCoO_2 after the heat-treatment step, from which the mechanisms of cycling and thermal performance enhancement may be developed.

It is hypothesized that the addition of a coating to the Li_xCoO_2 surface can modify the reactivity between active particles and the electrolyte, which can strongly influence its cycling performance and thermal characteristics. In this study, we focus on the following questions: (1) what is the microstructure of "$AlPO_4$"-coated $LiCoO_2$, particularly the coating microstructure; (2) how does its microstructure yield improved cycling and thermal stability; (3) how do lithium ions diffuse through the coating layer; and (4) why does the $AlPO_4$ coating chemistry yield superior cycling performance and thermal properties relative to other oxide coating materials. This work employs energy-dispersive X-ray spectroscopy (EDX) in a scanning transmission electron microscope (STEM) to obtain the distribution of Co, O, Al, and P on the micrometer- and nanometer-scale of the "$AlPO_4$"-coated $LiCoO_2$ powder sample, and uses X-ray photoelectron spectroscopy to analyze the chemical environments of C, Al, P, Co, O, and Li in order to provide new insights to the phases present on the surfaces of the active particles. In this paper, we show, for the first time, $AlPO_4$ is absent from the surfaces of the "$AlPO_4$"-coated $LiCoO_2$ particles. Li_3PO_4 and $LiCo_{1-y}Al_yO_2$ with relatively high Al substitution levels are detected on active particles. The mechanism by which the coating microstructure of "$AlPO_4$"-coated $LiCoO_2$ can lead to enhancement in cycle life and thermal stability relative to those of a uncoated $LiCoO_2$ sample is discussed.

Experimental Section

Bare $LiCoO_2$ and "$AlPO_4$"-coated $LiCoO_2$ powder samples were prepared as described previously.[19] Bare $LiCoO_2$ was prepared from stoichiometric amounts of Co_3O_4 and Li_2CO_3 at 1000 °C for 4 h in an oxygen stream. An $AlPO_4$ nanoparticle solution was prepared by slowly dissolving $Al(NO_3)_3 \cdot 9H_2O$ and $(NH_4)_2HPO_4$ in distilled water until a white $AlPO_4$ nanoparticle suspension was observed. The $AlPO_4$ nanoparticles with particle sizes in the range of 5−10 nm were amorphous, as determined by X-ray diffraction (XRD).[18] Bare $LiCoO_2$ was added to this suspension and mixed thoroughly for 5 min. The slurry was dried in an oven at 120 °C for 6 h and heat-treated at 700 °C for 5 h, from which the "$AlPO_4$"-coated $LiCoO_2$ was obtained. The weight fraction of $AlPO_4$ on $LiCoO_2$ is 1% after firing at 700 °C, as determined by inductively coupled plasma−mass spectroscopy (ICP−MS) (ICPS-1000IV, Shimadzu).

The reversible capacities and electrochemical activity of bare $LiCoO_2$ and "$AlPO_4$"-coated $LiCoO_2$ composite electrodes were measured in 2016 coin cells. Composite electrodes were prepared from electrode slurry, which was comprised of active material powder, poly vinylidene fluoride (PVDF), and Super P carbon black in an 80:10:10 weight ratio in *N*-methyl pyrrolidone (NMP) solution. The slurry was cast onto Al foil and dried under a vacuum at room temperature overnight, and subsequently dried under a vacuum at

(20) Cho, J. P.; Park, B. *J. Power Sources* **2001**, *92* (1−2), 35−39.
(21) Cho, J.; Kim, Y. J.; Park, B. *J. Electrochem. Soc.* **2001**, *148* (10), A1110−A1115.
(22) Fey, G. T. K.; Yang, H. Z.; Kumar, T. P.; Naik, S. P.; Chiang, A. S. T.; Lee, D. C.; Lin, J. R. *J. Power Sources* **2004**, *132* (1−2), 172−180.
(23) Fey, G. T. K.; Weng, Z. X.; Chen, J. G.; Lu, C. Z.; Kumar, T. P.; Naik, S. P.; Chiang, A. S. T.; Lee, D. C.; Lin, J. R. *J. Appl. Electrochem.* **2004**, *34* (7), 715−722.
(24) Chen, Z. H.; Dahn, J. R. *Electrochem. Solid-State Lett.* **2002**, *5* (10), A213−A216.
(25) Chen, Z. H.; Dahn, J. R. *Electrochem. Solid-State Lett.* **2004**, *7* (1), A11−A14.
(26) Kim, B.; Kim, C.; Kim, T. G.; Ahn, D.; Park, B. *J. Electrochem. Soc.* **2006**, *153* (9), A1773−A1777.

120 °C for 8−10 h. Fifteen millimeter diameter electrode disks were punched and redried under a vacuum at 120 °C for 30 min before being kept in an argon-filled glovebox. Coin cells were constructed inside the glovebox using a lithium metal foil as the negative electrode and the composite positive electrode separated by two polypropylene microporous separators (Celgard). The electrolyte used was 1 M $LiPF_6$ in a 1:1 weight ratio ethylene carbonate (EC): dimethyl carbonate (DMC) solvent (Merck or LithChem International). Assembled coin cells were allowed to soak overnight and then began electrochemical testing on a Solartron 1470 battery testing unit. Galvanostatic charging and discharging was performed at a *C*/50 rate (5.48 mA/g) to measure the voltage profiles of bare $LiCoO_2$ and "$AlPO_4$"-coated $LiCoO_2$ close to thermodynamic equilibrium. In addition, cycling performance of these samples was compared at a *C*/5 rate between voltage limits of 3.0 and 4.7 V vs Li for 30 cycles after the first cycle measured at a *C*/10 rate.

The particle morphology and surface microstructure of bare $LiCoO_2$ and "$AlPO_4$"-coated $LiCoO_2$ powder samples, which were sprinkled onto silver paint on an aluminum stub, were examined and imaged on a JEOL 6320FV field-emission scanning electron microscopy (SEM). In addition, transmission electron microscopy (TEM) was used to examine the cross-sectional microstructure of the coating layer on "$AlPO_4$"-coated $LiCoO_2$. TEM samples were prepared by embedding the "$AlPO_4$"-coated $LiCoO_2$ powder in a clear epoxy resin and then microtoming slices of 30 nm thickness. These cross-sections were examined on a JEOL 2010 transmission electron microscope under an accelerating voltage of 200 kV.

Powder XRD patterns of "$AlPO_4$"-coated $LiCoO_2$ samples were collected on a PANalytical X'Pert Pro X-ray diffractometer with CoK_α radiation. Data were collected between 10 and 140° of 2θ, at a scan rate of 0.167 °/min. The lattice parameters were determined using the HighScore Plus software package.

Elemental distributions of Co, Al, P, and O in "$AlPO_4$"-coated $LiCoO_2$ particles that were fractured in liquid nitrogen were collected using EDX spectroscopy in a VG HB603 STEM at room temperature, using a beam voltage of 250 kV and a beam diameter of ∼2 nm. Data collection times ranged from 3 to 10 min, depending on signal intensity for a given sample area.

Surface chemical compositions of bare $LiCoO_2$ and "$AlPO_4$"-coated $LiCoO_2$ were measured using X-ray photoelectron spectroscopy on a Physical Electronics model 5400 X-ray photoelectron spectrometer. The data were collected at room temperature, using a non-monochromatic Al K_α (1486.6 eV) X-ray source, with an angle of 45° between the analyzer and the X-ray source. The samples were mounted onto a gold-coated sample holder with the aid of electrically conducting tabs and placed into the introduction chamber, which was evacuated using roughing and turbomolecular pumps, for about 10−15 min before being transferred into the analysis chamber of the XPS instrument. Data collection proceeded when the analysis chamber pressure reached 2×10^{-8} Torr. The size of the analysis area was set to a 1.1 mm diameter spot. Survey spectra were collected at a low resolution using an analyzer pass energy of 89.45 eV, increment of 0.5 eV/step, and integration interval of 50 ms/step. The final spectrum consists of the average of 20 cycles. Multiplex spectra of various photoemission lines were collected at medium resolution using analyzer pass energy of 35.75 eV, increment of 0.2 eV/step, and an integration interval of 50 ms/step. Data collection intervals were approximately 37 min for survey spectra and ∼100−200 min for each set of multiplex spectra depending on sample composition. The linearity of the spectrometer energy scale was calibrated using the Au $4f_{7/2}$ and Cu $2p_{3/2}$ photoemission lines. The measured binding energies for these two lines were 83.93 and 932.59 eV, respectively, which compare well with the established values of 84.00 and 932.66 eV. The measured binding energies are shifted by −0.07 eV with respect to the established values. To compensate for this small shift and sample charging effects, all spectra were calibrated with the C 1s photoemission peak for adventitious hydrocarbons at 284.6 eV. Curve fit analysis of the photoemission lines was done using a combined Gaussian−Lorentzian line shape, except in the case of the Co $2p_{3/2}$ line where an asymmetric line shape was used, after subtracting a Shirley type background. For overall surface composition analysis, the atomic ratios of the relevant elements were determined from multiplex spectra using the integrated areas after subtracting the satellite contributions and a Shirley-type background and using the relative sensitivity factors provided by Physical Electronics for our spectrometer. The relative sensitivity factors for Li 1s, C 1s, O 1s, Co $2p_{3/2}$, Al 2s, P 2p, and Na 1s photoemission lines were given as 0.028, 0.312, 0.733, 2.113, 0.256, 0.525, and 1.102. It should be noted that the X-ray source and collection angle of 45° used in this experiment yield a sampling depth of ∼5 nm for the O 1s photoemission line.[27]

To identify the nature of the bonding environment on the coated $LiCoO_2$, we used aluminum phosphate ($AlPO_4$), layered O3 $LiAl_{0.1}Co_{0.9}O_2$, lithium carbonate (Li_2CO_3), gamma lithium phosphate (γ-Li_3PO_4), and layered O3 lithium aluminum oxide ($LiAlO_2$) as reference samples for the XPS studies. The X-ray powder diffraction patterns of these reference samples are shown in the Supporting Information (Figure S1).

Results and Discussion

Electrochemical Characterization. The galvanostatic voltage profiles of lithium coin cells having bare $LiCoO_2$ and ""$AlPO_4$"-coated $LiCoO_2$ electrodes are compared in Figure 1a. The "$AlPO_4$"-coated $LiCoO_2$ shows a voltage plateau at ∼3.93 V, characteristic of the insulator−metal transition,[28] a particular feature at ∼4.15 V, characteristic of monoclinic distortion associated with lithium and vacancy ordering,[29] and two distinct plateaus at ∼4.53 and ∼4.62 V, corresponding to the transitions from the O3 to the H1−3 phase, and the H1−3 to the O1 phase, respectively.[30] The voltages at which these plateaus occurred were reproducible to an accuracy of 0.01 V. In contrast, the voltage profile of bare $LiCoO_2$ is rather smooth, where the insulator−metal transition at ∼3.93 V and the monoclinic transition at ∼4.15 V were not found. These observations are in agreement with those of bare $LiCoO_2$ and "$AlPO_4$"-coated $LiCoO_2$ reported by Cho et al.[15] Levasseur et al. have reported that lithium overstoichiometry in $LiCoO_2$ having Li:Co ratios greater than 1.05 can suppress these phase transitions characteristic of stoichiometric $LiCoO_2$.[31] Therefore, it is hypothesized that the bare $LiCoO_2$ sample is lithium overstoichiometric, whereas the "$AlPO_4$"-coated $LiCoO_2$ sample largely consists of stoichiometric $LiCoO_2$, which will be further discussed in the context of XPS data in later sections. Moreover, it is

(27) Briggs, D.; Grant, J. T. *Surface Analysis by Auger and X-Ray Photoelectron Spectroscopy*; IM Publications and SurfaceSpectra Limited: Manchester, U.K., 2003; p 53.
(28) Menetrier, M.; Saadoune, I.; Levasseur, S.; Delmas, C. *J. Mater. Chem.* **1999**, *9* (5), 1135−1140.
(29) Shao-Horn, Y.; Levasseur, S.; Weill, F.; Delmas, C. *J. Electrochem. Soc.* **2003**, *150* (3), A366−A373.
(30) Chen, Z. H.; Lu, Z. H.; Dahn, J. R. *J. Electrochem. Soc.* **2002**, *149* (12), A1604−A1609.
(31) Levasseur, S.; Menetrier, M.; Suard, E.; Delmas, C. *Solid State Ionics* **2000**, *128* (1−4), 11−24.

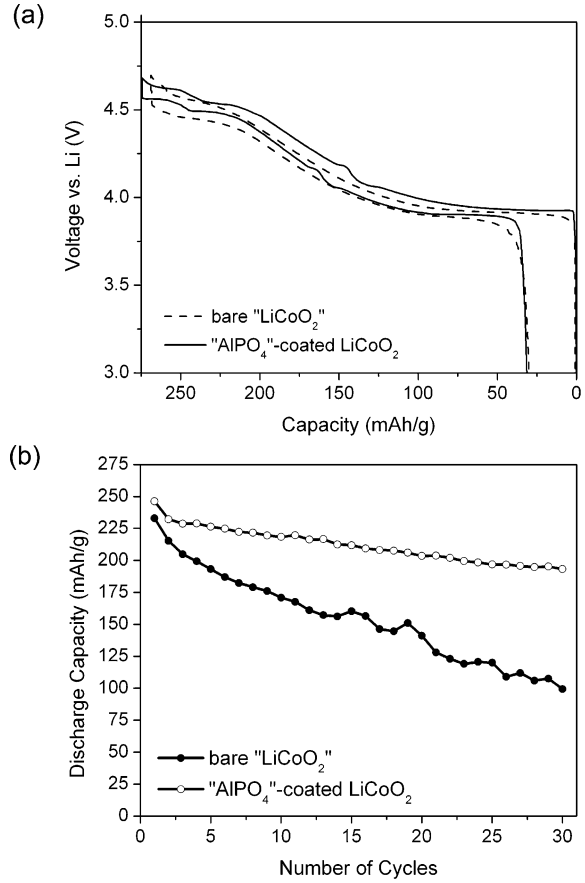

Figure 1. (a) First-cycle voltage profiles at *C*/50 show that bare $LiCoO_2$ is lithium-overstoichiometric, whereas the coated $LiCoO_2$ is stoichiometric, having a sharp, flat plateau at 3.93 V, lithium-vacancy ordering at $x = 0.5$, and distinct transitions to the H1−3 phase. (b) Capacity retention of bare and "$AlPO_4$"-coated $LiCoO_2$ for 30 cycles between voltage limits of 3.0 and 4.7 V. First cycle at *C*/10 rate, all subsequent cycles at a *C*/5 rate.

noted that "$AlPO_4$"-coated $LiCoO_2$ exhibits higher voltages of approximately 0.02 V upon charge and discharge relative to the bare $LiCoO_2$, as shown in Figure 1a. As Al substitution in $LiCoO_2$ has been shown to increase the equilibrium voltage for lithium insertion and removal,[7,32−34] it is postulated that a very small amount of Al substitution may exist in the bulk of the "$AlPO_4$"-coated $LiCoO_2$ sample. This speculation is in good agreement with previous findings[21] in that heating a mixture of 5 wt % Al_2O_3 nanoparticles and 95 wt % $LiCoO_2$ at 700 °C results in considerable Al substitution (5 at %) in $LiCoO_2$ (down to 100 nm from the particle surface).

Discharge capacities of bare $LiCoO_2$ and "$AlPO_4$"-coated $LiCoO_2$ upon cycling are compared in Figure 1b and have been shown to be repeatable within 10 mA h g^{-1}. After 30 cycles between the voltage limits of 3.0 and 4.7 V, the coated sample maintained 78.5% capacity retention compared to its first cycle, whereas the bare sample retained only 42.6% of its first-cycle capacity. The improvement in the capacity retention of "$AlPO_4$"-coated $LiCoO_2$ is in good agreement with previous studies.[14,15,17] In addition, it should be noted that impedance growth was much reduced in the lithium cells of cycled "$AlPO_4$"-coated $LiCoO_2$ relative to those of cycled bare electrodes (see the Supporting Information, Figure S2). Previous studies[35] have suggested that capacity loss is attributed to impedance growth during cycling to high voltage. Moreover, "$AlPO_4$"-coated $LiCoO_2$ electrodes in this study were shown to exhibit much better capacity retention relative to "ZrO_2"-coated $LiCoO_2$ electrodes[35] upon cycling to 4.7 V. This difference is not understood. It is speculated that "$AlPO_4$"-coated and "ZrO_2"-coated $LiCoO_2$ samples might have very different surface microstructures, which may strongly influence the cycling characteristics.

Microstructure Characterization−SEM and TEM Imaging. SEM secondary electron images of bare $LiCoO_2$ and "$AlPO_4$"-coated $LiCoO_2$ particles are compared in images a and b in Figure 2. The rounded morphology of bare $LiCoO_2$ particles is in good agreement with the hypothesis that bare $LiCoO_2$ is lithium overstoichiometric, as stoichiometric $LiCoO_2$ produced at high temperatures such as 1000 °C are typically platelike.[36] The surface of the bare $LiCoO_2$ particle appears to be fairly smooth, whereas most of the surface of "$AlPO_4$"-coated $LiCoO_2$ particles is rough. A fractured particle from the "$AlPO_4$"-coated $LiCoO_2$ sample shown in Figure 2c appears to suggest that (1) each particle is a single crystal and (2) a large number of small pits exist at the edge of what appear to be the basal $(003)_{hex}$ planes in comparison to the crystal surfaces parallel to the $(003)_{hex}$ planes. To gain further insight on the microstructure of "$AlPO_4$"-coated $LiCoO_2$, we performed TEM studies of microtomed "$AlPO_4$"-coated $LiCoO_2$ particles, where more than 15 different particles were examined to provide a representative picture of the microstructure. Typical cross-sectional TEM images of an "$AlPO_4$"-coated $LiCoO_2$ particle or crystal are shown in Figure 3, where reveals the microstructure of the outer edge of the particle. The coating layer appeared to cover most of the particle surface but it was found that the thickness was not uniform on the micrometer-scale with a thickness variation of 10−100 nm. This observation is repeatable over a number of particle cross-sections with intact surfaces that were studied. This observation is also consistent with the pitted surface found in the SEM images (Figure 2b). At the nanometer scale, an ∼10 nm surface layer is clearly visible (Figure 3), which is in good agreement with previous findings.[12]

Powder X-ray Diffraction Measurements. X-ray powder diffraction analyses showed that bare $LiCoO_2$ was single-phase, which can be indexed to the O3 layered structure with space group $R\bar{3}m$. Although the O3 layered phase was the major phase in the "$AlPO_4$"-coated $LiCoO_2$ sample, orthorhombic Li_3PO_4 in the γ-phase,[37] which can form at temperatures above 500 °C, was detected as a minor phase, as shown in the X-ray powder diffraction data in Figure 4. Evidence for the presence of $AlPO_4$ was not found in the diffraction data. The volume fraction of Li_3PO_4 is less than

(32) Julien, C. *Solid State Ionics* **2003**, *157* (1−4), 57−71.
(33) Ceder, G.; Aydinol, M. K.; Kohan, A. F. *Comput. Mater. Sci.* **1997**, *8* (1−2), 161−169.
(34) Ceder, G.; Chiang, Y. M.; Sadoway, D. R.; Aydinol, M. K.; Jang, Y. I.; Huang, B. *Nature* **1998**, *392* (6677), 694−696.
(35) Chen, Z. H.; Dahn, J. R. *Electrochim. Acta* **2004**, *49* (7), 1079−1090.
(36) Levasseur, S. Ph.D. Thesis, University of Bordeaux I, Pessac, France, 2002.
(37) Wang, B.; Chakoumakos, B. C.; Sales, B. C.; Kwak, B. S.; Bates, J. B. *J. Solid State Chem.* **1995**, *115* (2), 313−323.

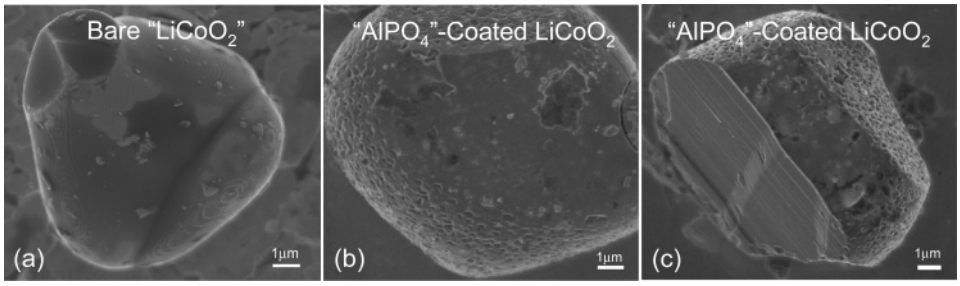

Figure 2. Scanning electron micrographs of (a) bare $LiCoO_2$ and (b) "$AlPO_4$"-coated $LiCoO_2$, showing the rounded shape of the particles. The coated sample shows a unique pitted texture on the side faces. (c) A fractured particle of "$AlPO_4$"-coated $LiCoO_2$ shows the layers of the bulk material oriented normal to the faces, which show a pitted surface texture.

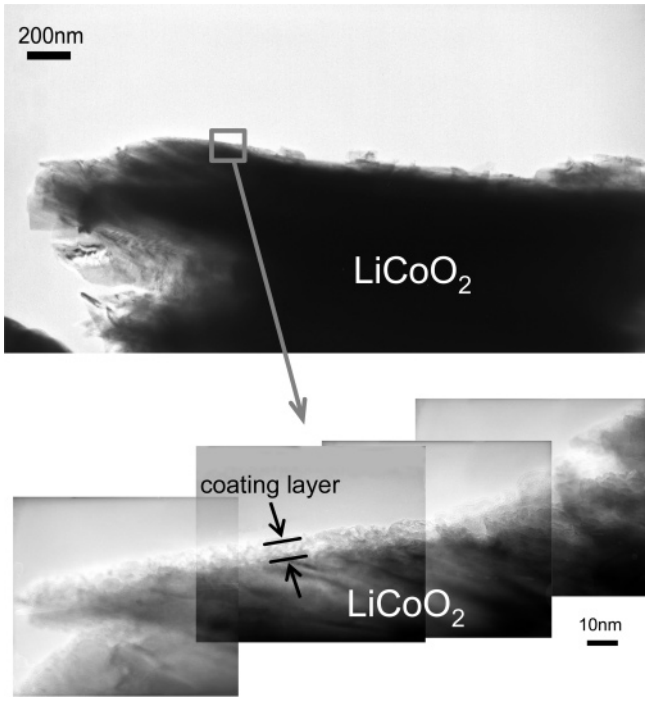

Figure 3. Cross-sectional TEM images of the "$AlPO_4$"-coated $LiCoO_2$ show uniform coverage of the particle surface, with a thickness variation of 10−100 nm. High-resolution TEM images of the coating cross-section show a light−dark variation which may indicate regions of varying composition or thickness in the coating.

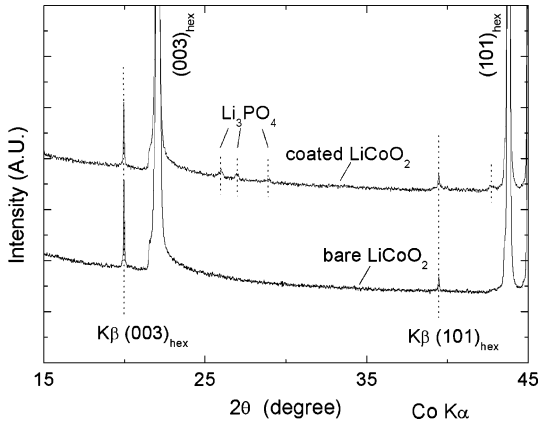

Figure 4. X-ray diffraction patterns of bare $LiCoO_2$ and "$AlPO_4$"-coated $LiCoO_2$ show the appearance of peaks corresponding to Li_3PO_4 in the coated sample.

1% in the "$AlPO_4$"-coated $LiCoO_2$ sample. Although the reactivity between $LiCoO_2$ and $AlPO_4$ thin films was found recently by Kim et al.,[26] this result revealed the first evidence of Li_3PO_4 formation in the "$AlPO_4$"-coated $LiCoO_2$ samples.

Table 1. Results of XPS Quantitative Analysis of Overall Surface Composition of Bare and Coated $LiCoO_2$[a]

	surface atomic concentration (%)	
element	bare $LiCoO_2$	"$AlPO_4$"-coated $LiCoO_2$
lithium (Li 1s)	18.6	18.3
cobalt (Co $2p_{3/2}$)	15.9	6.2
oxygen (O 1s)	50.5	50.3
ionically bonded	27.0	15.6
covalently bonded	23.5	34.7
aluminum (Al 2s)	0	6.7
phosphorus (P 2p)	0	2.5
carbon (C 1s)	13.6	14.1
adventitious	11.0	12.5
oxidized	2.6	1.6
Na 1s	1.4	1.9
Li:Co ratio	1.17	2.96
Al:P ratio	N/A	2.73

[a] Quantitative analysis was performed using high-resolution spectra of the photoemission lines listed in the table using CasaXPS software. Both peaks measured for O 1s were included in the analysis for each sample. Other elements consisted of a single peak for analysis. Satellite contributions were removed, and curve fitting analysis was used to eliminate interference between the Co 3p and Li 1s peaks.

Table 2. XRD Lattice Parameters and c_{hex}/a_{hex} Ratio of Bare $LiCoO_2$ and "$AlPO_4$"-Coated $LiCoO_2$ Reveal Negligible Differences between the Two Samples; Lattice Parameters Were Determined Using the HighScore Plus Software Package

	bare $LiCoO_2$	"$AlPO_4$"-coated $LiCoO_2$
a_{hex} (Å)	2.8152	2.8151
c_{hex} (Å)	14.0374	14.0430
c_{hex}/a_{hex}	4.986	4.988

It is believed that the $AlPO_4$ coating nanoparticles reacted with excess lithium in bare $LiCoO_2$ particles to form Li_3PO_4 on the particle surface and rendered stoichiometric $LiCoO_2$ in the bulk during the heat treatment at 700 °C. Upon Li_3PO_4 formation, remaining Al^{3+} may form $LiAlO_2$ or $LiCo_{1-y}Al_yO_2$ with high levels of Al substitution on the particle surface and diffuse into the particle interior to form $LiCo_{1-y}Al_yO_2$ solid solutions with small amounts of Al substitution.

The lattice parameters of the O3 layered structure in the bare $LiCoO_2$ and "$AlPO_4$"-coated $LiCoO_2$ samples are compared in Table 2. No significant difference was found between these samples. This observation is consistent with previous findings in that although lithium overstoichiometry leads to different voltage profiles, there is no correlation between lattice parameters and lithium overstoichiometry.[31]

STEM EDX Measurements of "$AlPO_4$"-Coated $LiCoO_2$. A bright-field STEM image and EDX elemental maps of Co, Al, P, and O collected from one particle are shown in Figure 5. Al and P maps clearly reveal that these two

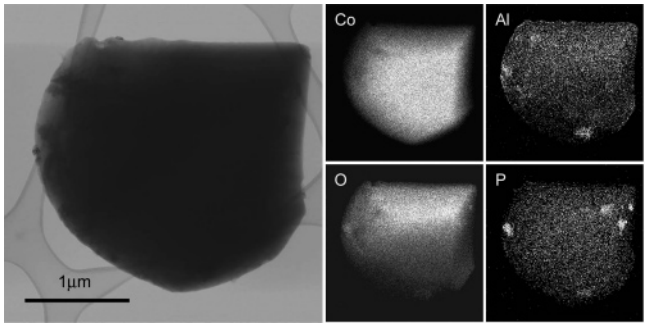

Figure 5. Energy-dispersive X-ray mapping on a cross-sectional piece of "$AlPO_4$"-coated $LiCoO_2$ shows the physical distribution of the Co, O, Al, and P. The aluminum signal is uniformly distributed in a thin surface layer to the particle edge; the phosphorus signal is more concentrated in smaller regions of nonuniformity.

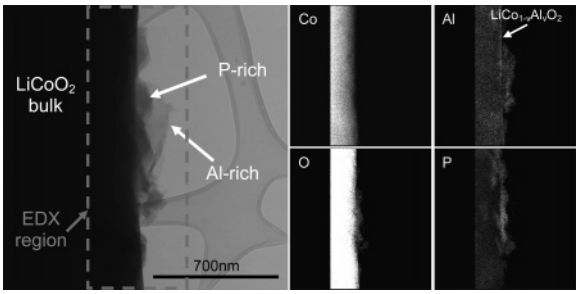

Figure 6. EDX mapping of "$AlPO_4$"-coated $LiCoO_2$ particle edge with STEM. Only the center region of the image has been mapped by EDX. Clearly, certain features correspond to phosphorus-rich clusters, whereas the aluminum seems more evenly distributed across the thick coating region and the rest of the particle surface. Oxygen distribution follows the phosphorus distribution most closely, and cobalt is confined to the particle bulk.

elements are not distributed uniformly over the whole particle. In addition, the intensities of Al and P do not show co-incident regions of high or low intensity, as would be expected if they occurred in a 1:1 atomic ratio of Al:P as in $AlPO_4$. Moreover, the intensity of Co signals increases from particle edge to particle center, which is expected from the increasing thickness toward the center under the transmitted electron beam. However, the aluminum signal appears strong and well-defined at the particle edge, which indicates that Al is not substituted uniformly in the "$AlPO_4$"-coated $LiCoO_2$ and is segregated on the particle surface in a thin layer. These observations indicate the formation of Al-rich regions and P-rich regions on the particle surface. A bright-field STEM image and EDX maps of another particle in Figure 6 clearly reveals the distinct separation of Al-rich regions and P-rich regions in the surface layer. It is interesting to note that Co was not detected in the Al-rich and P-rich regions. In addition, a thin white line was noted in the Al map, which may suggest the formation of a thin shell of O3 layered $LiCo_{1-y}Al_yO_2$ solid solution with high Al substitution levels. Moreover, the O signals corresponded closely to the same region as the P signals, indicating the presence of a compound containing both elements as in Li_3PO_4. The observations are in good agreement with the formation of Li_3PO_4 as revealed by XRD (Figure 4). Therefore, combined X-ray diffraction and STEM EDX data suggest that reactions between $AlPO_4$ nanoparticles and bare $LiCoO_2$ during the heat-treatment step lead to formation of Al-rich regions,

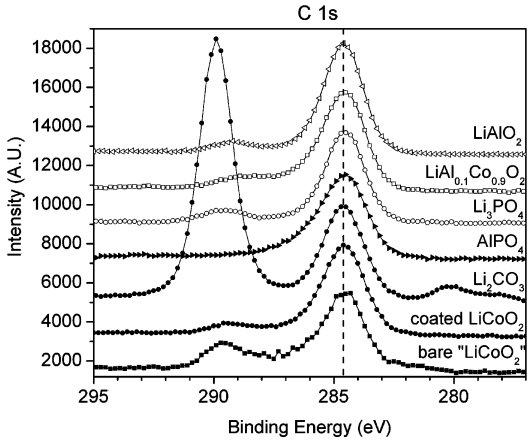

Figure 7. XPS spectra of the C 1s photoemission line for bare $LiCoO_2$ and "$AlPO_4$"-coated $LiCoO_2$ and some reference compounds. Dashed line shows location of hydrocarbon calibration peak at 284.6 eV.

namely, $LiCo_{1-y}Al_yO_2$ with high Al content, and P-rich regions, namely, Li_3PO_4, on the particle surface.

XPS Measurements of Bare $LiCoO_2$ and "$AlPO_4$"-Coated $LiCoO_2$. *Surface Chemical Compositions.* The surface chemical compositions of bare $LiCoO_2$ and "$AlPO_4$"-coated $LiCoO_2$ are compared in Table 1. The bare $LiCoO_2$ sample was found to have a surface composition of $Li_{19}Co_{16}O_{51}C_3$, with a Li:Co atomic ratio of ~1.17, which can be attributed to lithium-overstoichiometry of lithium cobalt oxide particles and lithium carbonate species on the surface. The presence of the high-binding-energy component of the C 1s line indicates that Li, in part, is present in the form of Li_2CO_3 on the particle surface. The overall surface composition includes only the measured quantity of oxidized portion of carbon in the form of Li_2CO_3 and excludes the hydrocarbon species. Quantitative analysis of "$AlPO_4$"-coated $LiCoO_2$ yielded an overall surface composition of $Li_{18}Co_6Al_7P_3O_{50}C_2$. The Li:Co atomic ratio increased significantly to 2.96 relative to bare $LiCoO_2$, which supports the hypothesis that some lithium (presumably in the form of Li_2CO_3) from the bare $LiCoO_2$ reacted with the $AlPO_4$ nanoparticles during the 700 °C heat treatment. As no significant Co was detected in the Al-rich and P-rich regions in the STEM EDX analysis (Figure 6), the detection of Co by XPS indicated that the surface of $LiCoO_2$ may not be covered completely by Al-rich and P-rich regions. Moreover, it should be noted that the surface atomic concentrations of aluminum (6.7%) and phosphorus (2.5%) are not in a one-to-one ratio, which is the ratio in the original $AlPO_4$ particles. This result of a higher Al surface concentration than P may suggest that Al-rich surface regions either in the form of $LiCo_{1-y}Al_yO_2$ or $LiAlO_2$ are thin and cover larger fractions of the particle surface relative to relatively thick P-rich regions in the surface coating layer.

Chemical Environments. Both bare $LiCoO_2$ and "$AlPO_4$"-coated $LiCoO_2$ samples were shown to have a broad peak near 289 eV for the C 1s photoemission line, as shown in Figure 7. As the pure Li_2CO_3 reference sample employed in this study shows a C 1s peak at 289.8 eV (with hydrocarbon calibration to 284.6 eV, and Dedryvere et al. have reported that the C 1s peak of Li_2CO_3 falls at 290.0 eV (with hydrocarbon calibration to 285.0 eV),[38] it is proposed that

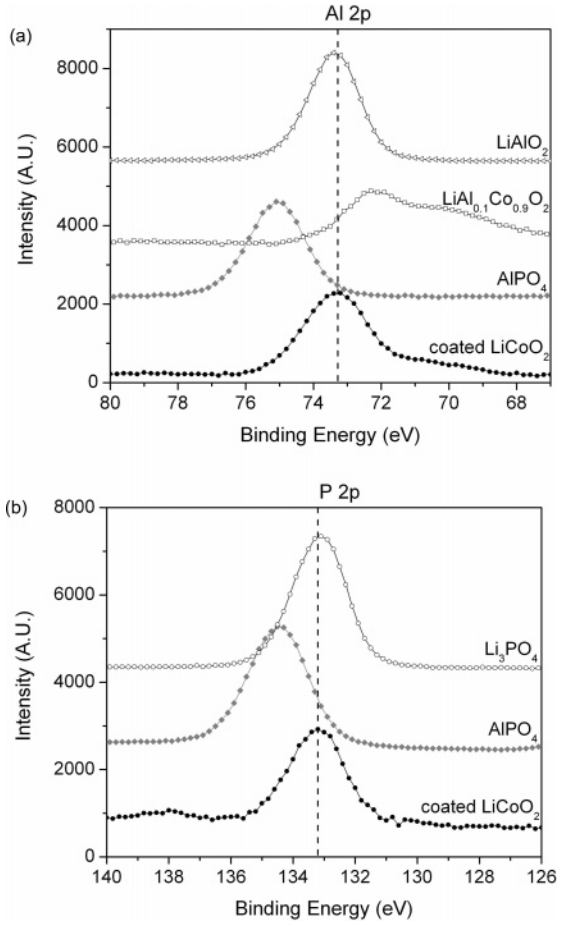

Figure 8. XPS spectra of the (a) Al 2p and (b) P 2p photoemission lines for "$AlPO_4$"-coated $LiCoO_2$ and pure $AlPO_4$. The large shifts to lower binding energy for the coated $LiCoO_2$ relative to the reference $AlPO_4$ for both spectra indicate that the aluminum and phosphorus are not present as $AlPO_4$ in the surface coating. The oxidation states of Al and P on the coated $LiCoO_2$ surface are similar to those of P in Li_3PO_4 and Al in $LiAlO_2$. Dashed lines indicate peak positions in the coated $LiCoO_2$ sample.

the oxidized C detected in both samples is in the form of Li_2CO_3. It should be noted that all the Li-containing samples examined in this study (Figure 7) exhibit the C 1s peak characteristic of Li_2CO_3. Therefore, it is believed that the presence of Li_2CO_3 on the particle surface results from surface reactions with CO_2 in air. It is also possible that a small fraction of this signal is due to Na_2CO_3 species, as indicated by a small Na signal in the survey spectrum. It was found that bare $LiCoO_2$ has significantly more surface Li_2CO_3 in comparison to "$AlPO_4$"-coated $LiCoO_2$. Quantitative comparison of C 1s peaks of carbonate species with the hydrocarbon calibration peaks revealed that the amount of carbonate species was reduced by about 70% for the coated $LiCoO_2$ compared to bare $LiCoO_2$.

The Al 2p and P 2p photoemission peaks were found for "$AlPO_4$"-coated $LiCoO_2$ but not for bare $LiCoO_2$, as expected. Here, we examine the binding environment of Al and P. As shown in Figure 8a, the Al 2p peak occurs at 73.3 eV. This peak position considerably differs from the Al 2p peak at 75.0 eV of the reference $AlPO_4$ sample used in this study and the reported value of 74.5 eV for the Al 2p in an

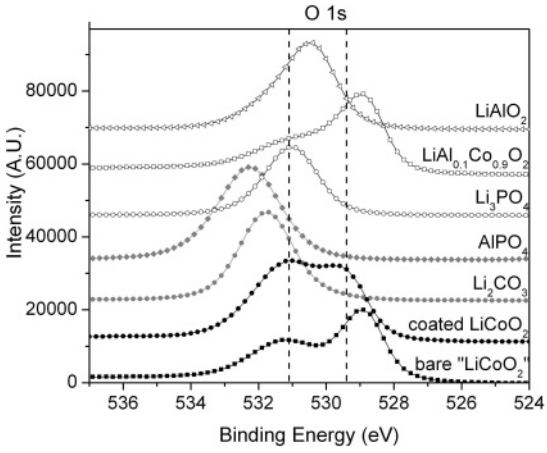

Figure 9. XPS spectra of the O 1s photoemission line for bare and coated $LiCoO_2$, in comparison with some reference compounds. The coated $LiCoO_2$ photoemission peak at 531.13 eV is distinctly different from that of the reference $AlPO_4$ sample at 532.22 eV. Dashed lines indicate the peak positions in the coated $LiCoO_2$ sample.

$AlPO_4$ thin film.[39] This difference further confirms that the $AlPO_4$ phase is absent from the particle surface of "$AlPO_4$"-coated $LiCoO_2$. Given a resolution of 0.05 eV for our XPS data, the Al 2p peak found in the "$AlPO_4$"-coated $LiCoO_2$ is comparable to that of the reference $LiAlO_2$ sample having an Al 2p peak at 73.4 eV but is higher than that of the reference Al-substituted $LiCoO_2$−$LiAl_{0.1}Co_{0.9}O_2$ sample (72.4 eV). This result is in good agreement with the view that the surface of the coating layer may contain Al-substituted $LiCoO_2$ with substitution levels that are much higher than that of $LiAl_{0.1}Co_{0.9}O_2$ and close to that of $LiAlO_2$. The P 2p photoemission peak at 133.2 eV for "$AlPO_4$"-coated $LiCoO_2$ is considerably different from that of the reference $AlPO_4$ at 134.4 eV but agrees very well with that of the reference Li_3PO_4 sample at 133.2 eV, as shown in Figure 8b. This result is consistent with the detection of orthorhombic Li_3PO_4 on the surface of "$AlPO_4$"-coated $LiCoO_2$ as revealed by X-ray powder diffraction data. Therefore, these comparative studies of Al 2p and P 2p binding energies confirm previous STEM EDX data that the coating layer contains no $AlPO_4$.

The O 1s photoemission lines from bare $LiCoO_2$ and "$AlPO_4$"-coated $LiCoO_2$ samples show two peaks, as shown in Figure 9. The lower-binding-energy peak at 528.9 eV for bare $LiCoO_2$ and 529.4 eV for "$AlPO_4$"-coated $LiCoO_2$ can be attributed to the O^{2-} ions in the O3 layered structure. It is speculated that the higher binding energy of O 1s line for "$AlPO_4$"-coated $LiCoO_2$ is attributed to Al substitution in $LiCoO_2$ on the particle surface, which makes the cobalt−oxygen bonds more covalent[40] and shifts the O 1s peak to higher binding energy relative to bare $LiCoO_2$. Dupin et al.[41] have shown that a $LiCoO_2$ sample prepared at 900 °C shows the O1s peak at 529.1 eV (with hydrocarbon calibration to the same energy as that used in this study). The slight shifts in the binding energy of O 1s of bare $LiCoO_2$ relative to

(38) Dedryvere, R.; Laruelle, S.; Grugeon, S.; Poizot, P.; Gonbeau, D.; Tarascon, J. M. *Chem. Mater.* **2004**, *16* (6), 1056−1061.

(39) Kim, B.; Kim, C.; Ahn, D.; Moon, T.; Ahn, J.; Park, Y.; Park, B. *Electrochem. Solid-State Lett.* **2007**, *10* (2), A32−a35.

(40) Castro-Garcia, S.; Castro-Couceiro, A.; Senaris-Rodriguez, M. A.; Soulette, F.; Julien, C. *Solid State Ionics* **2003**, *156* (1−2), 15−26.

(41) Dupin, J. C.; Gonbeau, D.; Martin-Litas, I.; Vinatier, P.; Levasseur, A. *J. Electron Spectrosc. Relat. Phenom.* **2001**, *120* (1−3), 55−65.

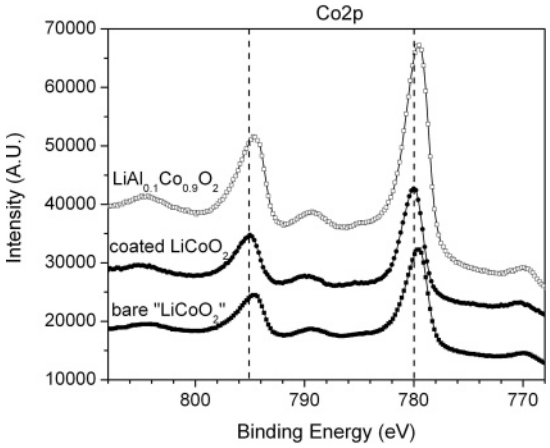

Figure 10. XPS spectra of the Co 2p photoemission lines for bare and coated $LiCoO_2$, with $LiAl_{0.1}Co_{0.9}O_2$ reference compound. The Co 2p photoemission peaks for coated $LiCoO_2$ are shifted by 0.4 eV to higher binding energy relative to bare $LiCoO_2$. Dashed lines indicate the peak positions in the coated $LiCoO_2$ sample.

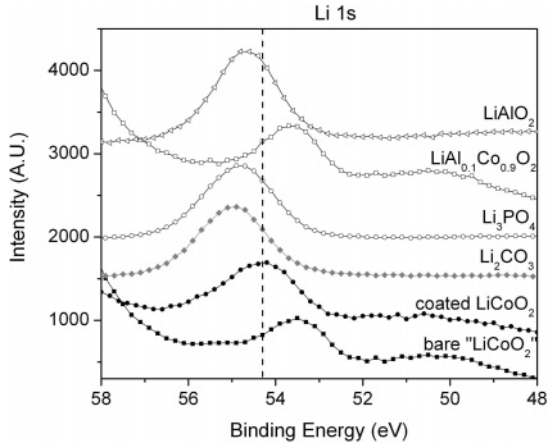

Figure 11. XPS spectra of the Li 1s photoemission line for bare and coated $LiCoO_2$ with some reference compounds. The coated $LiCoO_2$ shows a photoemission peak at 54.44 eV, which may contain contributions from Li_3PO_4 at 54.90 eV, and heavily Al-doped $LiCoO_2$, which would show a peak between that of 10%-Al-doped $LiCoO_2$ at 53.81 eV and that of $LiAlO_2$ at 54.69 eV. The dashed line indicates the peak position in the coated $LiCoO_2$ sample.

that of Dupin et al.[41] are not well-understood. The presence of Li_3PO_4 and $LiCo_{1-y}Al_yO_2$ (with high levels of Al substitution) phases in the surface layer can lead to shifts of the O 1s peak at ~529 eV to higher energy, as shown in Figure 9. The higher-binding-energy peaks of bare $LiCoO_2$ and "$AlPO_4$"-coated $LiCoO_2$ occur at 531.2 and 531.1 eV, respectively. This peak in the "$AlPO_4$"-coated $LiCoO_2$ sample can be attributed to the presence of Li_3PO_4 on the surface, as the Li_3PO_4 sample shows an O 1s peak at 531.1 eV. However, it is difficult to speculate the physical origin of this peak for the bare sample. Assuming all non-HC carbon peak is carbonate species, about 33.734% of this higher binding energy peak of O 1s results from carbonate species on the surface of bare $LiCoO_2$ particles, and other components such as surface defects have to be considered. Dupin et al. have suggested that such a peak might result from surface defects associated with oxygen oxidation greater than O^{2-} ions[41,42] and more covalent Co−O bonds[43] on the $LiCoO_2$ particle surface. Moreover, it should be noted that reference $AlPO_4$ shows an O 1s peak at 532.2 eV that is considerably different from the observed O 1s signals of "$AlPO_4$"-coated $LiCoO_2$, which further confirms that $AlPO_4$ is not present on the coated particle surface.

The Co 2p peaks for bare $LiCoO_2$ reveal a $2p_{1/2}$ peak and a $2p_{3/2}$ peak at 779.6 and 794.8 eV, respectively, as shown in Figure 10. Shakeup satellite peaks for each line are located at 10 eV higher relative to the main peak. These peak positions correspond well with those of Co^{3+} (779.6 and 794.8 eV) as reported by Dupin et al.[42] "$AlPO_4$"-coated $LiCoO_2$ shows $2p_{1/2}$ and $2p_{3/2}$ peaks with a shift of 0.4 eV toward higher binding energy relative to those of bare $LiCoO_2$ and $LiCo_{0.9}Al_{0.1}O_2$. The nature of this energy difference observed in the "$AlPO_4$"-coated $LiCoO_2$ sample is not understood, which may result from a dissimilar bonding environment of Co^{3+} in pyramidal sites induced by lithium-overstoichiometry[44] in the bare $LiCoO_2$ and $LiCo_{0.9}Al_{0.1}O_2$ or Co binding environments in $LiCo_{1-y}Al_yO_2$ with high levels of Al substitution approaching $LiAlO_2$ on the surface of "$AlPO_4$"-coated $LiCoO_2$ particles.

The Li 1s photoemission peak was measured at 53.8 and 54.4 eV for bare $LiCoO_2$ and "$AlPO_4$"-coated $LiCoO_2$, respectively, after removing Co 3p satellite contributions, as shown in Figure 11. This peak represents lithium in an octahedral environment of oxygen atoms of the O3 layered structure.[42] The considerable increase in lithium binding energy for "$AlPO_4$"-coated $LiCoO_2$ may result from contributions from other Li-containing phases present in the coating layer. For example, $LiAlO_2$ and Li_3PO_4 show a Li 1s peak at 54.7 and 54.9 eV, respectively. The value of the Li 1s peak position found for "$AlPO_4$"-coated $LiCoO_2$ fell in between that of $LiCoO_2$ and that of $LiAlO_2$, which is in good agreement with the presence of a heavily Al-substituted $LiCoO_2$ phase present on the particle surface.

Discussion

Proposed Microstructure for $AlPO_4$-Coated $LiCoO_2$. Charge and discharge voltage profiles have suggested that bare $LiCoO_2$ is lithium-overstoichiometric and XPS analyses have revealed that this sample has a Li:Co atomic ratio of 1.17. The high Li:Co ratio, in part, is due to the presence of surface Li_2CO_3 contaminant. The bare $LiCoO_2$ sample was mixed with 1 wt % $AlPO_4$ nanoparticles and heat-treated at 700 °C to form "$AlPO_4$"-coated $LiCoO_2$. In the "$AlPO_4$"-coated $LiCoO_2$ sample, the bulk layered structure appears to be lithium-stoichiometric, as evidenced by the presence of insulator−metal, lithium-vacancy ordering, and O3 to H1−3 transitions, although a small level of Al (<10 at. %) may be substituted in bulk during the heat-treatment step. Combined X-ray powder diffraction, STEM EDX, and XPS analyses of "$AlPO_4$"-coated $LiCoO_2$ have shown that (1) $AlPO_4$ is absent on the coated particle surface; (2) Al-rich

(42) Dupin, J. C.; Gonbeau, D.; Benqlilou-Moudden, H.; Vinatier, P.; Levasseur, A. *Thin Solid Films* **2001**, *384* (1), 23−32.
(43) Alcantara, R.; Ortiz, G. F.; Lavela, P.; Tirado, J. L.; Jaegermann, W.; Thissen, A. *J. Electroanal. Chem.* **2005**, *584* (2), 147−156.
(44) Levasseur, S.; Menetrier, M.; Shao-Horn, Y.; Gautier, L.; Audemer, A.; Demazeau, G.; Largeteau, A.; Delmas, C. *Chem. Mater.* **2003**, *15* (1), 348−354.

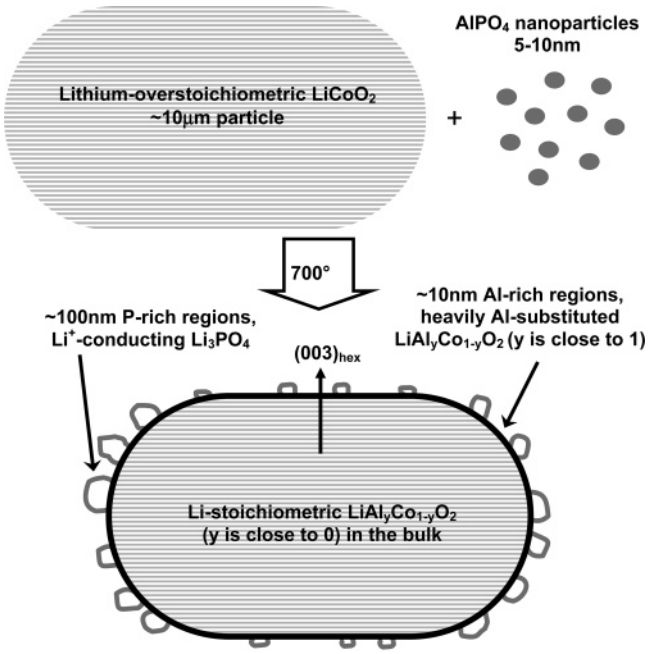

Figure 12. Proposed mechanism of coating structure and composition on $LiCoO_2$ surface after application of $AlPO_4$ nanoparticles and firing at 700 °C.

$LiAl_yCo_{1-y}O_2$ (y is close to 1) and P-rich Li_3PO_4 regions are present on the surface; and (3) surface coverage of Al-rich regions (~10 nm) is high but the thickness is small relative to P-rich regions (~100 nm). The proposed microstructure for "$AlPO_4$"-coated $LiCoO_2$ is shown in Figure 12. X-ray powder diffraction analyses have confirmed that Li_3PO_4 has an orthorhombic structure in the γ phase. In this study, we propose that excess lithium in the form of Li_2CO_3 in bare $LiCoO_2$ reacts with $AlPO_4$ nanoparticles during the heat treatment at 700 °C and produces a rough or pitted surface microstructure along the edges of the layers.

Implication of Coating Microstructure on Rate Capability and Cycling. Li_3PO_4 is a lithium ion conductor,[35,36] which would allow lithium diffusion through the coating during charge and discharge of "$AlPO_4$"-coated $LiCoO_2$. As it has a lithium ion conductivity of $\sim 6 \times 10^{-8}$ S/cm,[45] a 100 nm Li_3PO_4 layer would result in an area specific resistance of ~170 Ω/cm^2, which would lead to an electrode resistance of ~ 0.17 Ω for a typical porous electrode of 1000 cm^2_{true}/cm^2_{geo}. Moreover, XPS data in this study suggest that the amount of Li_2CO_3 on the "$AlPO_4$"-coated $LiCoO_2$ particle surface is much lower than that on the bare $LiCoO_2$ (Figure 7). Li_2CO_3 is not known to conduct lithium in bulk and can be highly resistive to lithium transport between the liquid electrolyte and active particles. Therefore, the presence of Li_3PO_4 in the particle surface of "$AlPO_4$"-coated $LiCoO_2$ can lower resistance of lithium diffusion through the particle surface and reduce electrode polarization relative to bare $LiCoO_2$, which would lead to the improvement in rate capability. Al substitution in $LiCoO_2$ is shown to increase the lattice parameter c_{hex} and interlayer spacing,[7] and this structural change is believed to be responsible for enhanced lithium diffusion in bulk $LiCo_{1-y}Al_yO_2$ particles by Myung et al.[6] However, as the amounts of Al substitution in the bulk of "$AlPO_4$"-coated $LiCoO_2$ particles are very small, the role of bulk Al substitution in enhancing the rate capability is believed to be minor.

We propose that surface $LiAl_yCo_{1-y}O_2$ (y is close to 1) and Li_3PO_4 particles of "$AlPO_4$"-coated $LiCoO_2$ can protect Li_xCoO_2 from harmful interactions with the electrolyte and from attack by trace amounts of HF and reduce cobalt dissolution, which is believed to largely contribute to impedance growth upon cycling to high voltages. The protective nature of surface $LiAl_yCo_{1-y}O_2$ (y is close to 1) is supported by previous findings of Myung et al.,[6] which have shown that Al substitution of up to 30 at % can significantly reduce cobalt dissolution in the electrodes charged to 4.5 V. It is interesting to mention that Cho et al. have reported that "$AlPO_4$"-coated $LiCoO_2$ exhibits a considerably lower amount of cobalt dissolution and superior stability upon cycling to 4.8 V relative to "Al_2O_3"-coated $LiCoO_2$.[15] It should be noted that the "Al_2O_3"-coated $LiCoO_2$[15,21] obtained from a heat treatment at 700 °C is shown to develop $LiCo_{1-y}Al_yO_2$ solid solutions (having y in the range of 0.05 to 0) near the particle surface.[21] Inferior capacity retention of "Al_2O_3"-coated $LiCoO_2$ to "$AlPO_4$"-coated $LiCoO_2$ may be attributed to (1) absence of cobalt-free surface particles to protect active Li_xCoO_2 particles and (2) cobalt and aluminum dissolution from $LiCo_{1-y}Al_yO_2$ having low levels of Al substitution.[20] Moreover, Pereira et al.[46] have reported that removal of surface Li_2CO_3 from lithium overstoichiometric $LiCoO_2$ has been shown to lower electrode impedance and enhance cycling performance at room temperature. Reduction of surface Li_2CO_3 in the "$AlPO_4$"-coated $LiCoO_2$ may thus contribute to markedly improved cycling performance relative to bare "$LiCoO_2$". Detailed studies are needed to elucidate the mechanism.

Lithium removal from "$AlPO_4$"-coated $LiCoO_2$ leads to all phase transitions (insulator−metal, lithium and vacancy ordering, and O3 to H1−3 transitions) known to stoichiometric $LiCoO_2$. In contrast, these transitions are absent in the bare $LiCoO_2$. Although these phase transitions may lead to structural damage and capacity loss, particularly at extremely high current densities,[47] it is believed that superior cycling characteristics of "$AlPO_4$"-coated $LiCoO_2$ to bare $LiCoO_2$ results largely from surface stability rather than structural stability upon cycling to high voltages.

Implication of Coating Microstructure on Thermal Properties. Highly delithiated Li_xCoO_2 with a large number of Co^{4+} is thermodynamically unstable. It can release oxygen gas by thermal decomposition at relatively low temperatures, and react with liquid electrolyte to cause gas generation. "$AlPO_4$"-coated $LiCoO_2$ has exhibited superior thermal and safety characteristics upon overcharging and high-temperature storage at highly charged states in comparison to bare $LiCoO_2$ and "Al_2O_3"-coated $LiCoO_2$ samples.[12,15] The notice-

(45) Yu, X. H.; Bates, J. B.; Jellison, G. E.; Hart, F. X. *J. Electrochem. Soc.* **1997**, *144* (2), 524−532.

(46) Pereira, N.; Matthias, C.; Bell, K.; Badway, F.; Plitz, I.; Al-Sharab, J.; Cosandey, F.; Shah, P.; Isaacs, N.; Amatucci, G. G. *J. Electrochem. Soc.* **2005**, *152* (1), A114−A125.

(47) Christensen, J.; Newman, J. *J. Solid State Electrochem.* **2006**, *10* (5), 293−319.

able difference in the thermal and safety characteristics of highly charged electrodes in the presence of electrolyte suggests that modification of particle surface microstructure can significantly alter the kinetics of reactions between active particles and electrolyte. Yu et al.[45] have shown that Li_3PO_4 thin films can be stable up to 6 V vs Li under impedance measurements and some decomposition occurs (possibly decomposes to $Li_4P_2O_7$) at 3.6 V vs Li from potentiodynamic measurements, where this discrepancy is not explained. It is hypothesized in this study that large potential gradients can develop in the Li_3PO_4 regions on the surface of "$AlPO_4$"-coated $LiCoO_2$ particles upon overcharging and thus reduce the potential experienced by Li_xCoO_2, from which the decomposition of liquid electrolyte and gas generation are significantly decreased. The lack of a lithium-conducting solid electrolyte layer on the particle surface would result in high potentials at the interface between particle surface and liquid electrolyte upon overcharging. Therefore, it is postulated that the presence of electrochemically stable, lithium-conducting phases on the particle surface may significantly improve the thermal characteristics of Li_xCoO_2 at high voltages. This hypothesis is further supported by the fact that "$AlPO_4$"-coated $LiCoO_2$ exhibits much improved thermal characteristics in comparison to $LiCoO_2$ with oxide coating materials,[12,15] where Li-conducting phases are unlikely to form on the particle surface during the heat-treatment step. Although small amounts of Al substitution in $LiCoO_2$ particles can effectively reduce cobalt dissolution and provide improved cycling performance, it is speculated that $Li_xAl_yCo_{1-y}O_2$ solid solutions may not lower the kinetics of reactions with electrolyte relative to Li_xCoO_2 at low Li contents. Therefore, it is believed that complete surface coverage of $LiCoO_2$ particles with a thin layer of lithium-conducting phases that are electrochemically stable at high voltages would lead to superior thermal characteristics relative to the "$AlPO_4$"-coated $LiCoO_2$ sample examined in this study, which consists of particles partially covered by Li_3PO_4.

Very recently, Lee et al.[48] have shown that "$LiCoPO_4$"-coated $LiCoO_2$ shows even better thermal characteristics relative to "$AlPO_4$"-coated $LiCoO_2$ particles during nail penetration tests at 4.4 V. Such improvement has been attributed to reduction in the amounts of surface Li_2CO_3 and LiOH in the "$LiCoPO_4$"-coated $LiCoO_2$ relative to "$AlPO_4$"-coated $LiCoO_2$. However, it is surprising to note that $LiCoPO_4$ can suppress reactions with the electrolyte upon cycling to high voltages (close to ~5 V) or during overcharging[13], as recent findings[49] have shown that lithium removal from olivine $LiCoPO_4$ leads to significant electrolyte decomposition, which results in capacity loss during cycling. Further microstructural studies are needed to reveal the physical nature of particle surface of "$LiCoPO_4$"-coated $LiCoO_2$.

(48) Lee, H.; Kim, M. G.; Cho, J. *Electrochem. Commun.* **2007**, *9* (1), 149−154.

(49) Bramnik, N. N.; Nikolowski, K.; Baehtz, C.; Bramnik, K. G.; Ehrenberg, H. *Chem. Mater.* **2007**, *19* (4), 908−915.

Conclusions

In this study, it is proposed that surface microstructure of active particles plays an important role in the cycling and thermal characteristics of lithium batteries, particularly upon cycling to high voltages. Superior cycling and thermal properties of "$AlPO_4$"-coated $LiCoO_2$ to bare $LiCoO_2$ is attributed largely to a difference in the surface microstructure rather than structural instability. Combined STEM EDX and XPS studies have revealed that $AlPO_4$ does not exist in the "$AlPO_4$"-coated $LiCoO_2$ sample treated with a 700 °C heating step. The surface of "$AlPO_4$"-coated $LiCoO_2$ consists of a Li_3PO_4 phase and a $LiAl_yCo_{1-y}O_2$ phase with high levels of aluminum. It is proposed that both phases can significantly reduce Co dissolution and impedance growth during cycling to high voltages, which leads to superior cycling performance relative to bare $LiCoO_2$. XPS studies have shown that the amount of surface Li_2CO_3 is much smaller on the "$AlPO_4$"-coated $LiCoO_2$ particles. Moreover, having Li-conducting phases such as Li_3PO_4 and $LiAl_yCo_{1-y}O_2$ on the particle surface instead of Li-blocking Li_2CO_3 can reduce resistance to lithium diffusion at the particle−electrolyte interface, which may lead to enhanced rate capability. Furthermore, it is postulated that the presence of electrochemically stable, lithium-conducting phases on the particle surface may reduce the potential experienced by Li_xCoO_2 and significantly improve the thermal characteristics of Li_xCoO_2 at high voltages. Last, this study shows the importance of understanding the surface microstructure of electrode materials in order to design and develop lithium batteries with cycling and thermal properties that can meet the demands of portable and transportation applications.

Acknowledgment. This work was supported in part by an MIT Pappalardo Fellowship, by the MRSEC Program of the National Science Foundation under Award DMR 02-13282 and the Assistant Secretary for Energy Efficiency and Renewable Energy, Office of FreedomCAR and Vehicle Technologies of the U.S. Department of Energy, under Contract DE-AC03-76SF00098 with the Lawrence Berkeley National Laboratory. A.N.M. acknowledges financial support by the Carderock Division of the Naval Surface Warfare Center's In-house Laboratory Independent Research Program administrated under ONR's Program Element 0601152N. The authors thank Jin Yi for performing high-resolution TEM studies, Anthony Garratt-Reed for STEM EDX measurements, and Naoaki Yabuuchi for the X-ray diffraction analyses. Fruitful discussion with Naoaki Yabuuchi is acknowledged.

Supporting Information Available: X-ray diffraction patterns for reference compounds; voltage profiles (PDF). This material is available free of charge via the Internet at http://pubs.acs.org.

CM0715390